

CHROMSYMP. 1988

## **Characterization of polymers by thermal field-flow fractionation**

MARTIN E. SCHIMPF

*Department of Chemistry, Boise State University, Boise, ID 83725 (U.S.A.)*

---

### ABSTRACT

Thermal field-flow fractionation (ThFFF) is a useful technique for separating complex polymer mixtures. The unique features of ThFFF make it applicable to many polymers that are difficult to characterize by conventional methods. Advances in channel design, spearheaded by work at the University of Utah's Field-Flow Fractionation Research Center, have recently culminated in the introduction of a commercially available instrument. Motivated by this progress, ThFFF is reviewed in this paper with an emphasis on implementation. Theories governing retention, zone dispersion and optimization are summarized. Procedures for obtaining accurate molecular-weight distributions on polymers are reviewed along with sample handling techniques. Also discussed is the application of ThFFF to studies of thermal diffusion in polymer solutions. The paper concludes with a discussion of current trends in the field.

---

### INTRODUCTION

Great strides have been made in the understanding, implementation, and optimization of thermal field-flow fractionation (ThFFF) since its introduction over 20 years ago<sup>1</sup>. In characterizing polymeric materials, ThFFF benefits from the open well-defined geometry of the separation channel. Polymer scientists have become increasingly aware of the advantages of ThFFF, catalyzing the recent introduction of a commercial instrument (FFFractionation, Salt Lake City, UT, U.S.A.).

In ThFFF, a temperature gradient is used to drive polymer components into slower flow regions near the cold wall (Fig. 1). This process, termed thermal diffusion, is opposed by ordinary (Fickian) diffusion. The resulting distribution of polymer concentration across the bullet-shaped velocity profile is governed by the balance of the two diffusional processes. Like all FFF subtechniques, movement of components down the channel toward the detector is determined by their mean steady-state position in the velocity profile.

The unique features of ThFFF give it several advantages over size-exclusion chromatography (SEC). The ThFFF channel is open and lacks a stationary phase.

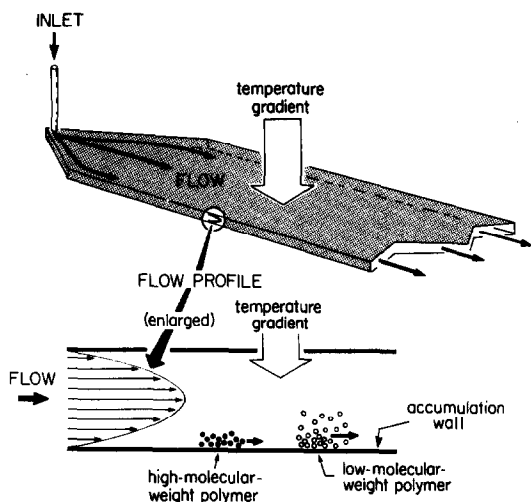


Fig. 1. Illustration of the principles of polymer separation by ThFFF (reprinted from ref. 44 courtesy of ACS Publications).

Thus, the flow profile of the carrier liquid and the dispersion of the sample zone are well characterized. Known equations relate zone retention and dispersion to transport coefficients of the polymer-carrier liquid system and to experimental parameters. These equations are used to compensate for zone dispersion in obtaining highly accurate information on molecular weight distributions (MWDs). The equations are also used to obtain values of the transport coefficients from retention data. Furthermore, they designate the experimental conditions that optimize individual separation problems. The unique channel features also provide excellent separation reproducibility; in the separation of  $>90$  polymers in 7 solvents using the same instrument, both retention and zone broadening were highly consistent<sup>2-4</sup>. Finally, retention volume, limited to one column volume in SEC, is theoretically unlimited in ThFFF (for practical reasons, however, retention volume is limited to approximately 20 channel volumes). This feature offers the ability to separate significantly more components in a single mixture (large peak capacity).

Among the factors that influence retention in ThFFF is the magnitude of the externally applied temperature gradient. This can be varied rapidly and precisely to accommodate molecular weights from 1000 (ref. 5) to  $>20 \cdot 10^6$  (ref. 6). By changing the temperature gradient continuously (programming), polymer mixtures containing components with a wide range in molecular weight can be handled in a single run<sup>7</sup>. While retention is also governed by the molecular weight of the polymer, the additional influence of chemical composition gives ThFFF an added dimension not present in SEC. This is illustrated in Fig. 2, which compares the resolving power of ThFFF and SEC on two polymers of similar molecular weight but varying chemical composition. The polymers coelute with SEC but are resolved by ThFFF because of differences in chemical composition.

Finally, separation in ThFFF is gentle; there is no interfacial transport or strong shear gradients. Thus, ThFFF is an ideal tool for characterizing fragile molecules such as high-molecular-weight polymers.

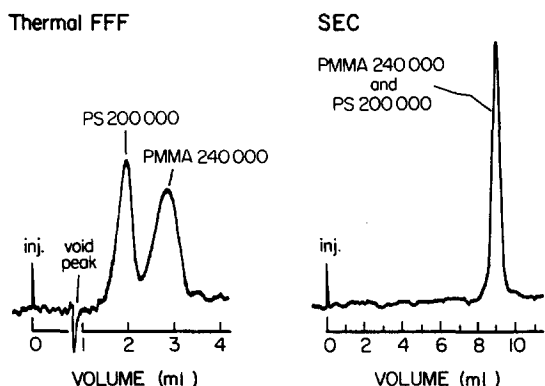


Fig. 2. Elution profiles of  $2.0 \cdot 10^5$  MW polystyrene (PS) and  $2.4 \cdot 10^5$  MW poly(methyl methacrylate) (PMMA) by ThFFF and SEC (reprinted from ref. 20 courtesy of Pergamon Press).

This paper reviews the application of ThFFF for characterizing polymers. Additional discussions on the conceptual basis and implementation of FFF and ThFFF are contained elsewhere<sup>8-21</sup>.

## THEORY

ThFFF theory is well-developed and has been described in a number of papers<sup>22-32</sup>. Summarized below are theories relevant to the understanding and implementation of ThFFF.

### Retention

The opposing forces of thermal and ordinary diffusion result in an exponential profile in polymer concentration, with decreasing concentration away from the cold wall (coordinate  $x$ ). The center of mass of the concentration profile is defined by its distance  $l$  from the cold wall. For mathematical convenience, parameter  $l$  is expressed in the dimensionless form  $\lambda = l/w$ , where  $w$  is the channel thickness. Retention parameter  $\lambda$  is related to the transport coefficients by

$$\lambda = \frac{D}{wD_T(dT/dx)} \quad (1)$$

where  $dT/dx$  is the temperature gradient across the channel, and  $D$  and  $D_T$  are the ordinary and thermal diffusion coefficients, respectively, of the polymer-carrier liquid system.

As in chromatography, the extent to which an analyte component is retained in FFF can be specified by the "retention ratio"  $R$ , defined as

$$R = \frac{V^0}{V_r} \quad (2)$$

where  $V^0$  is the volume of the channel and  $V_r$  is the volume of carrier liquid required to elute the component. By considering the profiles across the channel of both analyte component and carrier-liquid velocity,  $R$  can be related to retention parameter  $\lambda$ . Values of  $\lambda$ , computed from experimental  $R$  values, are used to calculate transport coefficients from eqn. 1. Accurate values of  $\lambda$  are also crucial in establishing the column dispersion function, as discussed below.

For most FFF subtechniques the shape of the velocity profile is parabolic, and the dependence of  $R$  on  $\lambda$  is

$$R = 6\lambda(\coth \frac{1}{2\lambda} - 2\lambda) \quad (3)$$

In ThFFF the temperature gradient and attendant carrier-liquid viscosity changes in the channel result in a velocity profile that is skewed, with maximum flow shifted toward the hot wall. Motivated by the need for accurate  $\lambda$  values the following relation between  $R$  and  $\lambda$  was derived<sup>28</sup>, accounting for the skewed velocity profile:

$$R = \frac{1}{\sum_{i=1}^5 \frac{h_i}{(i+1)}} \left\{ \frac{1}{(1 - e^{-1/\lambda})} \left[ \sum_{i=1}^5 h_i \sum_{j=0}^{i-1} \frac{i!}{(i-j)!} \lambda^j \right] + \sum_{i=1}^5 i! h_i \lambda^i \right\} \quad (4)$$

Parameters  $h_i$  are defined as

$$h_1 = \theta b_0 \quad (5a)$$

$$h_2 = (b_0 + \theta b_1)/2 \quad (5b)$$

$$h_3 = (b_1 + \theta b_2)/3 \quad (5c)$$

$$h_4 = (b_2 + \theta b_3)/4 \quad (5d)$$

$$h_5 = b_3/5 \quad (5e)$$

where

$$\theta = \left( \frac{b_0}{2} + \frac{b_1}{3} + \frac{b_2}{4} + \frac{b_3}{5} \right) / \left( b_0 + \frac{b_1}{2} + \frac{b_2}{3} + \frac{b_3}{4} \right) \quad (6)$$

and parameters  $b_i$  are defined as

$$b_0 = a_0 + a_1 T_c \quad (7a)$$

$$b_1 = a_1 S \quad (7b)$$

$$b_2 = -\frac{1}{2K_c} (dK/dT) a_1 S^2 \quad (7c)$$

$$b_3 = \frac{1}{2} \left( \frac{1}{K_C} \frac{dK}{dT} \right)^2 a_1 S^3 \quad (7d)$$

Here  $T_C$  is the cold wall temperature,  $K_C$  is the thermal conductivity of the carrier liquid at the cold wall,  $dK/dT$  is the rate of change in thermal conductivity with temperature, and

$$S = \Delta T + \frac{1}{K_C} \frac{dK}{dT} \frac{(\Delta T)^2}{2} \quad (8)$$

where  $\Delta T$  is the temperature difference between the hot and cold walls. Parameters  $a_0$  and  $a_1$  are the linear least-squares-fit parameters that describe the dependence of carrier-liquid fluidity,  $1/\eta$ , on temperature according to

$$\frac{1}{\eta} = a_0 + a_1 T \quad (9)$$

The relationship between  $R$  and  $\lambda$  can be significantly altered in accounting for the temperature dependence of viscosity. Fig. 3 compares the dependence of  $R$  on  $\lambda$  according to eqn. 4 (for a specific case) with the isoviscous dependence (eqn. 3).

#### Zone broadening

Dispersion of a solute band in FFF and chromatography is characterized by plate height  $H$ , the variance of the band relative to the distance traveled. The major contributions to plate height in ThFFF have been studied in detail<sup>29-34</sup>. The dispersion of a monodisperse sample is represented by the channel or column contribution to plate height  $H_C$ . For a polydisperse polymer, there is in addition to column dispersion, a selective dispersion arising from the tendency of the higher-molecular-weight species to migrate behind the lower-molecular-weight species. This polydispersity contribution is represented by  $H_p$ . Thus, the observed plate height is the sum of the two terms

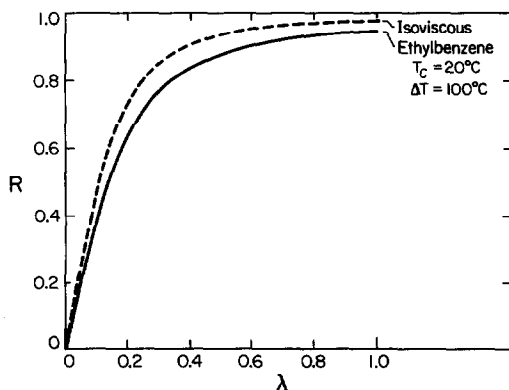


Fig. 3. Retention ratio  $R$  as a function of  $\lambda$  for the isoviscous system (eqn. 3) and ethylbenzene at  $T_C = 20^\circ\text{C}$  and  $\Delta T = 100^\circ\text{C}$ , according to eqn. 4.

$$H = H_p + H_c \quad (10)$$

For narrow MWDs, the polydispersity contribution is approximated by<sup>29</sup>

$$H_p = LS_M^2(\mu - 1) \quad (11)$$

where  $L$  is the channel length,  $\mu$  is the polydispersity, and  $S_M$  is the mass-based selectivity, defined as the dependence of retention volume  $V_r$  on molecular weight  $M$  according to

$$S_M = \frac{d \log V_r}{d \log M} \quad (12)$$

Zone dispersion in ThFFF is usually dominated by polydispersity ( $H_p \gg H_c$ ) because of the open channel geometry and high resolving power inherent to ThFFF. However, column dispersion is significant when characterizing ultra-narrow polymer standards. Column dispersion is also significant for broad MWDs when high carrier-liquid flows are used to shorten analysis time. For ThFFF,  $H_c$  is described by

$$H_c = H_D + H_N + H_R + H_{EC} \quad (13)$$

The first term on the right side of eqn. 13 accounts for broadening due to longitudinal diffusion. This term generally is negligible because of the slow diffusion of macromolecules. The second term on the right is the non-equilibrium (mass transfer) term. This term arises because sublayers of the sample zone are displaced unequally by the non-uniform velocity profile. Under appropriate conditions, the non-equilibrium term dominates column dispersion in ThFFF. The third term on the right accounts for dispersion that occurs while the sample zone is "relaxing" to its steady state profile at the accumulation wall after injection. During relaxation, the zone is briefly subjected to a greater than normal range of longitudinal flow velocities. While this term is usually negligible, it can be significant at high carrier-liquid velocities. Relaxation effects can be avoided by using a stop-flow procedure in which flow is halted during relaxation<sup>29</sup>. The last term in eqn. 13 accounts for the influence of extra-channel volume on plate height. This unwanted effect can be kept negligible by using minimum lengths of narrow-bore tubing between the sample valve and channel head, and between the channel outlet and detector cell. Large-volume detector cells must also be avoided.

The non-equilibrium contribution to plate height  $H_N$  is expressed as<sup>22</sup>

$$H_N = \frac{\chi w^2 \langle v \rangle}{D} \quad (14)$$

where  $\langle v \rangle$  is the average carrier-liquid velocity and  $\chi$  is a complicated function of  $\lambda$  and  $R$ <sup>34</sup>. Martin and Giddings<sup>23</sup> developed an approximation for  $\chi$  based on a third-degree polynomial expression for the velocity profile with one adjustable parameter  $v$ . The resulting equation for  $\chi$  is

$$\chi = \frac{2\lambda^2 F}{R(1 - e^{-1/\lambda})} \quad (15)$$

Here

$$F = 2A[6(1+v) - (1/\lambda) - (A/\lambda) + 36v\lambda^2 - 6\lambda(1+6v) + 18\lambda e^{-1/\lambda}(1+10v\lambda)] + 72\lambda^2[(1+v)^2 - 10\lambda(1+4v+3v^2) + 4\lambda^2(7+69v+90v^2) - 672v\lambda^3(1+3v) + 4464v^2\lambda^4] - 72\lambda^2 e^{-1/\lambda}[7 - 2v + v^2 + 2\lambda(5 - 68v + 15v^2) + 4\lambda^2(7 - 69v + 180v^2) - 672v\lambda^3(1 - 3v) + 4464v^2\lambda^4] \quad (16)$$

and

$$A = 12\lambda e^{-1/\lambda}(6v\lambda - 1)/(1 - e^{-1/\lambda}) \quad (17)$$

The value of  $v$  corresponding to the skewed velocity profile present in ThFFF can be approximated by<sup>32</sup>

$$v = \frac{h_1}{6 \sum_{i=1}^5 \frac{h_i}{(i+1)}} - 1 \quad (18)$$

Substitution of eqn. 15 into eqn. 14 yields

$$H_N = \frac{2F\lambda^2 w^2 \langle v \rangle}{RD(1 - e^{-1/\lambda})} \quad (19)$$

Previous studies<sup>29,32</sup> confirm that column dispersion in ThFFF is dominated by non-equilibrium dispersion which is accurately defined by eqns. 14–19. When characterizing narrow polymer samples,  $H_N$  can be simply subtracted from the overall plate height, and polydispersity information calculated from eqn. 11. In the separation of polydisperse samples, however, column dispersion cannot be accounted for by a single value of  $H_C$  because  $H_C$  varies with retention volume. To account for column dispersion in the separation of polydisperse samples, the following column dispersion function was derived<sup>32</sup>:

$$G(V, V_r) = \frac{V^0}{2wV_r} \left( \frac{D_T(1 - e^{-1/\lambda})\Delta T}{\lambda\pi FV_r \langle v \rangle Bw} \right)^{\frac{1}{2}} \times \exp \left[ \frac{-(V - V_r)^2 D_T (V^0)^2 (1 - e^{-1/\lambda}) \Delta T}{4\lambda FV_r^3 \langle v \rangle Bw^3} \right] \quad (20)$$

Here  $B$  is the channel breadth and  $V$  is the volume of carrier liquid eluting through the channel. Eqn. 20 defines the volume-based response of non-equilibrium dispersion as a function of retention volume  $V_r$ . By deconvoluting this function from a ThFFF fractogram<sup>32</sup>, the “ideal” elution profile is obtained. Here “ideal” refers to the elution profile that would be obtained if all dispersion in the channel were molecular-weight selective, directly reflecting the MWD.

Most polymer samples have relatively broad MWDs. The development of deconvolution methods for removing column dispersion was motivated by the goal of shortening the time required to analyze broad polymers without losing accuracy in the resulting MWD. Temperature programming, discussed in detail below, is another way to achieve this goal. By decreasing the temperature throughout the run, analysis time is

reduced without introducing column dispersion associated with increasing the carrier-liquid flow-rate.

## METHODOLOGY

### *Instrumentation*

The experimental apparatus for ThFFF is similar to that for high-performance liquid chromatography (HPLC) except for the channel itself. Equipment consists of a pump to drive the carrier liquid, the separation channel, and a detector and chart recorder to monitor the column eluent. Samples are injected with a microsyringe or injection valve. A computer can be used for data analysis and to control operating conditions, such as the temperature gradient across the channel.

The basic design of the ThFFF channel is illustrated in Fig. 4. It consists of two copper or copper alloy bars with highly polished chrome-plated faces. The bars are clamped together over a Mylar® spacer that has been cut out to form the channel. The thickness of the channel is typically 2–10 mils (51–127  $\mu\text{m}$ ). Thinner channels result in less column dispersion and higher speeds of analysis, while thicker channels can accommodate greater sample loads. Holes are drilled in each bar, at opposite ends, to form the inlet and outlet for the channel. The bars are sandwiched between boards of insulating material and the whole assembly is clamped together between aluminum plates.

The top bar is heated with electrical cartridge heaters; heat is removed from the bottom bar by circulating coolant through holes that run the length of the bar. Crude temperature control ( $\pm 2^\circ\text{C}$ ) of the hot bar can be achieved by controlling the power to the heaters with a voltage control device. More precise control ( $\pm 0.1^\circ\text{C}$ ) is possible by cycling the heaters on and off using computer-controlled relay switches. The cold-wall temperature is controlled by adjusting the flow of coolant through the bottom bar. The temperature difference established between the bars is generally from 5 to  $80^\circ\text{C}$ , with higher values applicable to lower molecular weight polymers.

Like HPLC, ThFFF is commonly used in connection with a concentration-sensitive detector, such as a refractometer or UV photometer. These can be paired with other detectors to provide additional information on polymers. For example, a continuous viscosity detector and refractometer have been coupled to provide information on the inherent viscosity distribution of polymers<sup>35</sup>. This characterization

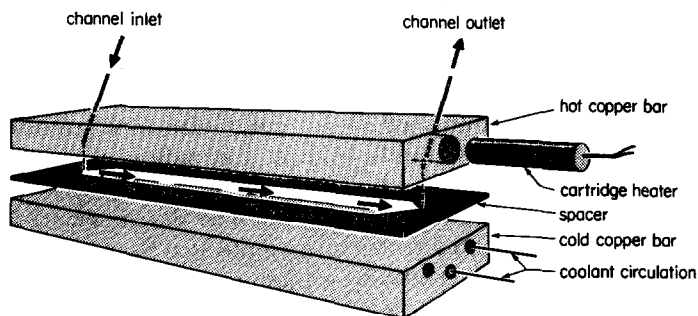


Fig. 4. Basic design of ThFFF channel.



property is often more directly relevant to end use than are MWD data. The use of a light-scattering photometer as a ThFFF detector has also been studied<sup>36</sup>.

### *Sample loading*

Transport coefficients vary with polymer concentration. Since these changes affect the retention ratio, it is important to use a range of polymer concentrations when measuring retention-derived parameters (such as  $D$ ). Values are then extrapolated to zero concentration for accurate definition. The effect of polymer concentration on transport coefficients is particularly strong near the critical concentration, where polymer solutions undergo an abrupt transition from "dilute" to "semidilute" behavior<sup>37</sup>. When the polymer zone in the ThFFF channel is near the critical concentration, overloading effects are observed<sup>38</sup>. Sample overloading in ThFFF generally is accompanied by peak "fronting" and a shift toward higher retention volumes. Excessive overloading gives rise to additional peaks at higher retention volumes, probably due to polymer aggregation. Whenever overloading is suspected the sample should be run at more than one concentration, and the individual fractograms should be examined for consistency in retention volume and peak shape.

The mass of polymer that can be injected without overloading increases with the solvating power of the carrier liquid and with the thickness of the channel; the maximum amount is also inversely proportional to the molecular weight and sample concentration. Thus when overloading is a concern, it is better to inject a large volume at low concentration than to inject a small volume at high concentration<sup>38</sup>.

### *Signal enhancement using splitters*

The analysis of high-molecular-weight polymers ( $> 1 \cdot 10^6$ ), requires the use of dilute solutions ( $< 1$  mg/ml) to prevent overloading. If the MWD is broad, the required concentration may be too dilute to be detected because the eluting zone is spread over a wide range in retention volume. To overcome this problem, the concentration of the sample in the detector can be increased with the use of a stream splitter<sup>39</sup>. A stream splitter divides the carrier flowstream at the outlet end of the channel such that the concentrated sample layer near the accumulation wall is split away from the bulk of the carrier stream. The concentrated sample stream is routed to the detector for a greatly enhanced signal.

### *Temperature programming*

Selectivity  $S_M$  is relatively constant for  $R > 0.3$ , but decreases rapidly<sup>40</sup> as  $R$  approaches 1. To optimize the resolution of all components in a polymer sample, the field strength must be sufficient to retain each component for at least three channel volumes. When separating polymer samples that span a broad molecular weight range, the field strength required to sufficiently retain the lowest-molecular-weight component may lead to excessive retention times of higher-molecular-weight species. Therefore, it is prudent to program the temperature gradient, beginning at a high value and decreasing continuously during the run. The initial high-temperature gradient optimally resolves the low-molecular-weight components; as the gradient drops to lower values the high-molecular-weight components are resolved.

A variety of mathematical functions have been used to program a decreasing temperature gradient. In the first report of temperature programming<sup>41</sup>, Giddings *et*

*al.* used a time-delay parabolic decay function to separate nine polymers ranging in molecular weight from 4000 to  $7.1 \cdot 10^6$ . The use of a linear function was also reported in this work. An exponential decay function developed by Kirkland and co-workers<sup>42,43</sup> produces a linear calibration plot of  $\log M$  vs. retention time. More recently, Giddings *et al.*<sup>44</sup> have reported the development of a power function for programming temperature gradients in ThFFF.

In power programming the field strength  $S_T$  is changed with time  $t$  according to the function

$$S_T = S_T^0 \left( \frac{t_1 - t_a}{t - t_a} \right)^p \quad (21)$$

where  $S_T^0$  is the initial field strength,  $t_a$  is an arbitrary time constant,  $t_1$  is the predecay time between the start of the run and the beginning of decay, and  $p$  is the decay power. These parameters are subject to the constraints  $t \geq t_1 > t_a$  and  $p > 0$ . When  $p = 2$  and  $t_a = -2t_1$ , the fractionating power (defined as the resolution of two components divided by their relative difference in molecular weight) is nearly independent of molecular weight. A constant fractionating power is desirable when highly polydisperse samples are characterized. Fig. 5 illustrates the use of power programming to separate 7 polymers ranging in molecular weight from 9000 to  $5.5 \cdot 10^6$ .

#### OPTIMIZATION

The greatest accuracy in measurements of MWDs can be obtained by maximizing the ratio  $P$  of the polydispersity plate-height contribution to the non-equilibrium contribution. Parameter  $P$  is equivalent to the square of the resolution between molecular-weight components located at  $\pm 2$  standard deviations from the mean of the MWD. Using eqns. 11 and 14,  $P$  can be written in the following form

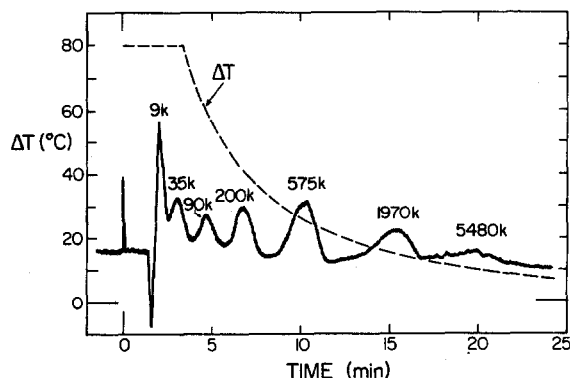


Fig. 5. Separation of 7 polymers of indicated molecular weights (in thousands, k) by power-programmed ThFFF (reprinted from ref. 44 courtesy of ACS Publications).

$$P = \frac{H_P}{H_N} = \frac{LS_M^2(\mu - 1)}{\chi w^2 \langle v \rangle / D} \quad (22)$$

If  $\chi$  is approximated<sup>34</sup> as  $24\lambda^3$ , and  $\lambda$  by  $R/6$  (ref. 45), then

$$P = \frac{9LS_M^2(\mu - 1)D}{w^2 R^3 \langle v \rangle} \quad (23)$$

Parameter  $P$  increases with the ratio  $L/\langle v \rangle$ . Although channel length  $L$  (typically about 50 cm) is fixed, flow-rates can be reduced to increase the accuracy of MWDs or the resolution between components. However, this has the simultaneous effect of increasing run time. Thus, a trade-off exists between accuracy or resolution, and speed. This situation is illustrated in Fig. 6, where the resolution between two components from five- and one-minute separations (in the same channel) is compared<sup>46</sup>. The former shows superior resolution but takes longer. The reduced resolution of the latter results from the proportionality of  $H_N$  to the mean carrier-liquid velocity  $\langle v \rangle$ .

Eqn. 23 shows that retention ratio  $R$  and channel thickness  $w$  are the most effective optimization parameters. For highest resolution, channel thickness should be minimized while the temperature gradient is maximized to reduce  $R$ . The cost of using thinner channels is reduced sample capacity. Lower  $R$  values increase run time, and temperature programming is used to optimize this trade-off. In characterizing industrial polymers, temperature programming is often essential to achieving accurate MWDs in a reasonable time.

## APPLICATIONS

ThFFF has been applied to a wide variety of lipophilic polymers, including polystyrene<sup>1-7,29,32-35,41-46</sup>, poly(methyl methacrylate)<sup>3,47,48</sup>, polyisoprene<sup>3,47,48</sup>, poly(tetrahydrofuran)<sup>47</sup>, polypropylene<sup>49</sup>, polyethylene<sup>49</sup> and nitrocellulose<sup>50</sup>. Al-

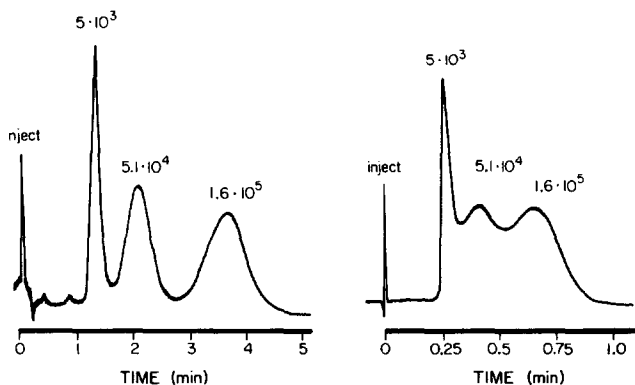


Fig. 6. Illustration of trade-off between resolution and speed in the separation of a three-component mixture of polystyrenes by ThFFF. Experimental conditions:  $\Delta T = 60^\circ\text{C}$ ,  $w = 51 \mu\text{m}$ , and  $\langle v \rangle = 0.56 \text{ cm/s}$  (left) or  $3.05 \text{ cm/s}$  (right) (reprinted from ref. 20 courtesy of Pergamon Press).

though thermal diffusion is generally weak in aqueous systems<sup>33,45,51</sup>, some non-ionic materials such as poly(ethylene oxide), poly(vinyl pyrrolidone) and poly(ethylene glycol) are sufficiently retained in water to permit characterization<sup>52</sup>. The advantages of ThFFF are particularly suited to the analysis of very-high-molecular-weight polymers, copolymers and polymers that interact with surfaces. Polymers needing corrosive solvents or high temperatures for solvation, and narrow-MWD polymers that require an accurate determination of polydispersity are also well handled by ThFFF. With the introduction of an instrument into the commercial marketplace, ThFFF is now being used for routine polymer analysis in several laboratories.

### *Polymer characterizations*

ThFFF currently relies on a calibration curve to relate molecular weight to retention volume. When the temperature gradient is held constant, calibration curves take the following form

$$\log V_r = S_M \log M \quad (24)$$

where  $S_M$  is the selectivity defined by eqn. 12. ThFFF is more accurate than SEC for measuring MWDs because selectivity in ThFFF is higher (typical  $S_M$  values are in the range 0.5–0.6) and column dispersion is well-defined. The high degree of accuracy of ThFFF has been clearly demonstrated in its application to polymer standards<sup>29,32</sup>.

When characterizing narrow polymer fractions, polydispersity is obtained from  $H_P$  using eqn. 11. Accurate values of  $H_P$  are obtained by subtracting  $H_N$  from the plate height of the elution profile, provided  $H_r$  is negligible. To obtain  $H_N$  from eqn. 19, the diffusion coefficient of the polymer fraction and several carrier-liquid parameters are required. If these values are unavailable,  $H_P$  can be determined by plotting plate height versus flow velocity. If  $H_r$  is negligible, a linear plot will be obtained with  $H_P$  as the intercept. Fig. 7 shows such a plot for a narrow polystyrene standard<sup>29</sup>. On the right-hand side of this plot, the ordinate is expressed in terms of  $\mu - 1$ , illustrating that any  $\mu$  value significantly above 1.01 can be unambiguously ruled out. This is much smaller than the ceiling value of 1.06 determined by the supplier using SEC. The plot in Fig. 7 has a high degree of linearity and the slope is within 3% of its theoretical value, suggesting that the value  $\mu = 1.003$  is reasonably accurate.

With broad MWDs, column dispersion is negligible when low flow-rates are used. If column dispersion is significant, it can be removed by deconvolution to obtain the "ideal" elution profile. To obtain the MWD  $m(M)$ , the fractogram or "ideal" elution profile is transformed using the following equation<sup>53</sup>

$$m(M) = c(V_r) \frac{dV_r(M)}{dM} \quad (25)$$

where  $c(V_r)$  is the detector trace of the mass-based concentration  $c$  (if a mass-sensitive detector is used); the scale factor  $[dV_r(M)/dM]$  is related to the selectivity by

$$\frac{dV_r}{dM} = \frac{V_r}{M} S_M \quad (26)$$

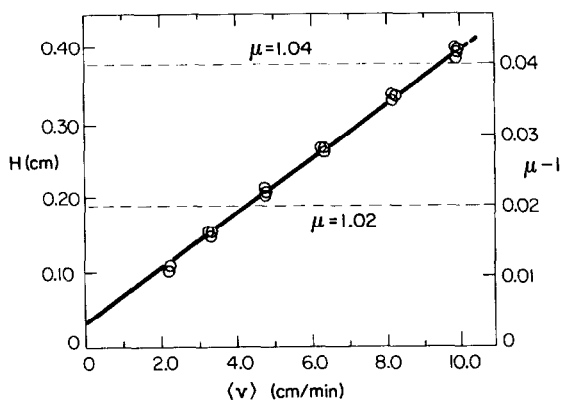


Fig. 7. Plot of plate height vs. flow velocity for a  $1.7 \cdot 10^5$  MW polystyrene sample illustrating polydispersity value  $\mu = 1.003$  (reprinted from ref. 20 courtesy of Pergamon Press).

### Thermal diffusion studies

Separation in ThFFF is governed by differences in the ordinary and thermal diffusion coefficients of polymer components. Although the underlying physicochemical parameters important to ordinary diffusion are well understood, those governing the thermal diffusion of polymers in solution are less clear. By increasing our understanding of thermal diffusion, and its dependence on polymer properties, we gain access to more information on polymers through ThFFF. Theories on the thermal diffusion of polymers in solution vary widely in conceptual basis and often predict contradictory results; experimental data lack consistency and wide applicability, partly due to the difficulty of conventional methodology. Fortunately, ThFFF is capable of producing accurate values of thermal diffusion parameters in polymer solutions, making it the best technique for the systematic study of thermal diffusion and thus of its own foundations.

In the first of a three-part study of thermal diffusion in polymer solutions, the ThFFF retention of a variety of linear and branched polystyrenes was examined with ethylbenzene as the carrier liquid<sup>2</sup>. A linear dependence of retention parameter  $\lambda$  on diffusion coefficient  $D$  was found, as illustrated in Fig. 8. According to eqn. 1, the slope of this plot is  $(wD_T dT/dx)^{-1}$ . Since  $w$  and  $dT/dx$  were identical for all runs, the constant slope demonstrates that  $D_T$  is independent of both polymer size and branching configuration.

Next,  $D_T$  values were obtained for 17 polymer-solvent systems<sup>3,54</sup>. The results were used to search for correlations between  $D_T$  and physiochemical parameters of the polymer and carrier liquid.  $D_T$  was found to be inversely proportional to the viscosity and solvating power of the carrier liquid. These correlations have been supported in similar studies by Kirkland *et al.*<sup>55</sup>.  $D_T$  was also found to increase with polymer density and with the thermal conductivity difference of the polymer and carrier liquid.  $D_T$  also correlates inversely with the activation energy of the solvent viscous flow<sup>3</sup>.

In the third part of the study<sup>4</sup>, the thermal diffusion of several copolymers in toluene was characterized. For random copolymers,  $D_T$  values apparently assume the weighted average of the corresponding homopolymer values, where the weighting

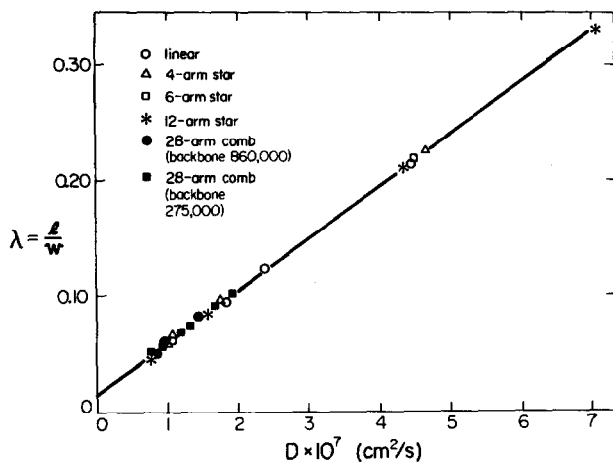


Fig. 8. Illustration of linear dependence of  $\lambda$  on diffusion coefficient  $D$  (reprinted from ref. 2 courtesy of ACS Publications).

factors are the mole-fractions of each monomer type in the copolymer. For block copolymers subject to radial segregation of their monomers, thermal diffusion appears to be dominated by monomers located in the outer (free-draining) regions of the solvated polymer molecule.

#### TRENDS

Interest in ThFFF has surged in recent years with the need for new techniques to better characterize an expanding variety of polymeric materials. Since the introduction of a commercial instrument, the application of ThFFF to routine polymer analysis is growing. As awareness of its unique features continue to increase, ThFFF will be applied with increasing frequency to polymers that are difficult to characterize accurately by traditional methods.

More work is needed to clarify the utility of ThFFF in characterizing copolymers. The studies referenced above suggest that the analysis of random copolymers is straightforward. However, additional work must be done to confirm these indications. The retention of block copolymers in ThFFF appears more complex; fundamental studies of copolymer retention continue.

The time required to resolve two polymer components by ThFFF continues to decrease. This is primarily the result of using thinner channels, although for broad MWDs, temperature programming has also contributed significantly to this trend. According to eqn. 23, for each two-fold reduction in channel thickness, the carrier velocity can be increased by a factor of four without losing resolution. Channels designed for high flow velocity are currently made with a thickness of  $76 \mu\text{m}$ , but thinner channels will become routine as channel surfaces are made smoother by improved techniques<sup>56</sup>. Channel thickness will ultimately be limited by detector sensitivity since thinner channels require lower sample concentrations to avoid overloading.

## SYMBOLS

$a$	coefficient of fluidity dependence on temperature
$A$	term defined by eqn. 17
$b$	term defined by eqn. 7
$B$	channel breadth
$c$	concentration
$D$	diffusion coefficient
$D_T$	thermal diffusion coefficient
$F$	term defined by eqn. 16
$G$	non-equilibrium dispersion function
$h$	term defined by eqn. 5
$H$	plate height
$H_C$	column dispersion contribution to plate height
$H_D$	longitudinal diffusion contribution to plate height
$H_{EC}$	extra-column volume contribution to plate height
$H_N$	non-equilibrium contribution to plate height
$H_P$	polydispersity contribution to plate height
$H_R$	relaxation contribution to plate height
$K$	carrier-liquid thermal conductivity
$K_C$	carrier-liquid thermal conductivity at the cold-wall temperature
$l$	altitude of the center of gravity of the analyte zone above the accumulation wall
$L$	channel length
$m(M)$	molecular weight distribution
$M$	molecular weight
$p$	power programming decay power
$P$	optimization ratio $H_P/H_N$
$R$	retention ratio $V^0/V_r$
$S$	term defined by eqn. 8
$S_M$	mass-based selectivity
$S_T$	field strength
$S_T^0$	initial field strength in temperature programming
$t$	time
$t_1$	predecay-time constant in power programming
$t_a$	decay-time constant in power programming
$T$	temperature
$T_C$	cold-wall temperature
$v$	velocity profile term defined by eqn. 18
$\langle v \rangle$	average velocity of the carrier liquid in the channel
$V$	elution volume
$V^0$	void volume of the channel
$V_r$	retention volume
$w$	channel thickness
$x$	altitude above the accumulation (cold) wall
$\Delta T$	temperature drop across the channel
$\eta$	viscosity

$\theta$	term defined by eqn. 6
$\lambda$	retention parameter $l/w$
$\mu$	polydispersity
$\chi$	non-equilibrium coefficient

## REFERENCES

- 1 G. H. Thompson, M. N. Myers and J. C. Giddings, *Sep. Sci. Technol.*, 2 (1967) 797–800.
- 2 M. E. Schimpf and J. C. Giddings, *Macromolecules*, 20 (1987) 1561–1563.
- 3 M. E. Schimpf and J. C. Giddings, *J. Polym. Sci., Polym. Phys. Ed.*, 27 (1989) 1317–1332.
- 4 M. E. Schimpf and J. C. Giddings, *J. Polymer Sci., Polym. Phys. Ed.*, in press.
- 5 J. C. Giddings, L. K. Smith and M. N. Myers, *Anal. Chem.*, 47 (1975) 2389–2394.
- 6 Y. S. Gao, K. D. Caldwell, M. N. Myers and J. C. Giddings, *Macromolecules*, 18 (1985) 1272–1277.
- 7 J. C. Giddings, L. K. Smith and M. N. Myers, *Anal. Chem.*, 48 (1976) 1587–1592.
- 8 J. C. Giddings, S. R. Fisher and M. N. Myers, *Am. Lab. (Fairfield, Conn.)*, 10 (1978) 15–31.
- 9 J. C. Giddings, M. N. Myers, K. D. Caldwell and S. R. Fisher, in D. Glick (Editor) *Methods of Biochemical Analysis*, Vol. 26, Wiley, New York, 1980, pp. 79–136.
- 10 E. N. Lightfoot, A. S. Chiang and P. T. Noble, *Annu. Rev. Fluid Mech.*, 13 (1981) 351.
- 11 J. C. Giddings, *Anal. Chem.*, 53 (1981) 1170A–1175A.
- 12 J. C. Giddings, M. N. Myers and K. D. Caldwell, *Sep. Sci. Technol.*, 16 (1981) 549–575.
- 13 J. C. Giddings, K. A. Graff, K. D. Caldwell and M. N. Myers, in C. D. Craver (Editor), *Advances in Chemistry Series*, No. 203, American Chemical Society, Washington, DC, 1983, Ch. 14, pp. 257–269.
- 14 T. Hoshino, *Bunseki*, 12 (1985) 856–864.
- 15 J. Janca, *Chem. Listy*, 81 (1987) 1034–1057.
- 16 J. C. Giddings, *Chem. Eng. News*, 66 (1988) 34–48.
- 17 K.-G. Wahlund, *Eur. Chrom. News*, 2 (1988) 12–15.
- 18 K. D. Caldwell, *Anal. Chem.*, 60 (1988) 959A–971A.
- 19 J. C. Giddings, *J. Chromatogr.*, 470 (1989) 327–335.
- 20 J. J. Gunderson and J. C. Giddings, in C. Booth and C. Price (Editors), *Comprehensive Polymer Science, Vol. 1, Polymer Characterization*, Pergamon, Oxford, 1989, pp. 279–291.
- 21 M. Martin and P. Reynaud, *Anal. Chem.*, 52 (1980) 2293.
- 22 J. C. Giddings, *J. Chem. Phys.*, 49 (1968) 81–85.
- 23 M. Martin and J. C. Giddings, *J. Phys. Chem.*, 85 (1981) 727–733.
- 24 J. C. Giddings, M. R. Schure, M. N. Myers and G. R. Velez, *Anal. Chem.*, 56 (1984) 2099–2104.
- 25 J. M. Davis and J. Calvin Giddings, *Sep. Sci. Technol.*, 20 (1985) 699–724.
- 26 J. C. Giddings, *Anal. Chem.*, 58 (1986) 735–740.
- 27 M. Martin and A. Jaulmes, *Sep. Sci. Technol.*, 16 (1981) 691.
- 28 J. J. Gunderson, K. D. Caldwell and J. C. Giddings, *Sep. Sci. Technol.*, 19 (1984) 667–683.
- 29 M. E. Schimpf, M. N. Myers and J. C. Giddings, *J. Appl. Polym. Sci.*, 33 (1987) 117–135.
- 30 L. K. Smith, M. N. Myers and J. C. Giddings, *Anal. Chem.*, 49 (1977) 1750–1756.
- 31 M. Martin, M. N. Myers and J. C. Giddings, *J. Liq. Chromatogr.*, 2 (1979) 147–164.
- 32 M. E. Schimpf, P. S. Williams and J. C. Giddings, *J. Appl. Polym. Sci.*, 37 (1989) 2059–2076.
- 33 M. E. Hovingh, G. E. Thompson and J. C. Giddings, *Anal. Chem.*, 42 (1970) 195–203.
- 34 J. C. Giddings, Y. H. Yoon, K. D. Caldwell, M. N. Myers and M. E. Hovingh, *Sep. Sci. Technol.*, 10 (1975) 447–460.
- 35 J. J. Kirkland, S. W. Rementer and W. W. Yau, *J. Appl. Polym. Sci.*, 38 (1989) 1383–1395.
- 36 M. Martin, *Chromatographia*, 15 (1982) 426–432.
- 37 P. G. DeGennes, *Macromolecules*, 9 (1976) 594.
- 38 K. D. Caldwell, S. L. Brimhall, Y. Gao and J. C. Giddings, *J. Appl. Polym. Sci.*, 36 (1988) 703–719.
- 39 J. C. Giddings, H. C. Lin, K. D. Caldwell and M. N. Myers, *Sep. Sci. Technol.*, 18 (1983) 293–306.
- 40 J. J. Gunderson and J. C. Giddings, *Anal. Chim. Acta*, 189 (1986) 1–15.
- 41 J. C. Giddings, L. K. Smith and M. N. Myers, *Anal. Chem.*, 48 (1976) 1587–1592.
- 42 J. J. Kirkland and W. W. Yau, *Macromolecules*, 18 (1985) 2305–2311.
- 43 J. J. Kirkland, S. W. Rementer and W. W. Yau, *Anal. Chem.*, 60 (1988) 610–616.
- 44 J. C. Giddings, V. Kumar, P. S. Williams and M. N. Myers, in C. D. Craver and T. Provder (Editors), *Polymer Characterization by Interdisciplinary Methods*, American Chemical Society, Washington, DC, in press.



- 45 M. N. Myers, K. D. Caldwell and J. C. Giddings, *Sep. Sci. Technol.*, 9 (1974) 47–70.
- 46 J. C. Giddings, M. Martin and M. N. Myers, *J. Chromatogr.*, 158 (1978) 419–435.
- 47 J. C. Giddings, M. N. Myers and J. Janca *J. Chromatogr.*, 186 (1979) 37–44.
- 48 J. J. Gunderson and J. C. Giddings, *Macromolecules*, 19 (1986) 2618–2621.
- 49 S. L. Brimhall, M. N. Myers, K. D. Caldwell and J. C. Giddings, *Sep. Sci. Technol.*, 16 (1981) 671–689.
- 50 M. E. Schimpf, S. L. Brimhall and J. C. Giddings, *Thermal Field-Flow Fractionation of Nitrocellulose*, Report to USAAMCCOM - LCWSL, University of Utah, Salt Lake City, UT, October 25, 1985.
- 51 F. J. Bonner, *Chem. Scr.*, 3 (1973) 149.
- 52 J. J. Kirkland and W. W. Yau, *J. Chromatogr.*, 353 (1986) 95–107.
- 53 J. C. Giddings, M. N. Myers, F. J. F. Yang and L. K. Smith, in M. Kerker (Editor), *Mass Analysis of Particles and Macromolecules by Field-Flow Fractionation, Colloid and Interface Science*, Vol. IV, Academic Press, New York, 1976, pp. 381–398.
- 54 M. E. Schimpf and J. C. Giddings, presented at the *192nd National ACS Meeting, Anaheim, CA, September 1986*.
- 55 J. J. Kirkland, L. S. Boone and W. W. Yau, presented at *1st International Symposium on Field-Flow Fractionation, Park City, UT, June 15, 1989*.
- 56 J. C. Giddings, K. D. Caldwell and L. F. Kesner, in A. R. Cooper (Editor), *Molecular Weight Determination (Chemical Analysis Series, Vol. 103)*, Wiley-Interscience, New York, 1989, Ch. 12.